

## Perturbative color transparency in electroproduction experiments

Bijoy Kundu,<sup>1,\*</sup> Jim Samuelsson,<sup>2,†</sup> Pankaj Jain,<sup>1,‡</sup> and John P. Ralston<sup>3,§</sup>

<sup>1</sup>*Department of Physics, IIT Kanpur, Kanpur-208 016, India*

<sup>2</sup>*Department of Theoretical Physics, Lund University, Sweden*

<sup>3</sup>*Department of Physics and Astronomy, University of Kansas, Lawrence, Kansas 66045*

(Received 2 February 1999; revised manuscript received 7 July 2000; published 7 November 2000)

We calculate quasi-exclusive scattering of a virtual photon and a proton or pion in nuclear targets. This is the first complete calculation of “color transparency” and “nuclear filtering” in perturbative QCD. The calculation includes full integrations over hard interaction kernels and distribution amplitudes in Feynman- $x$  fractions and transverse spatial separation space  $b$ . Sudakov effects depending on  $b$  and the momentum transfer  $Q^2$  are included. Attenuation of the hadronic states propagating through the medium is calculated using an eikonal Glauber formalism. Nuclear correlations are included explicitly. We find that the color transparency ratio is comparatively insensitive to theoretical uncertainties inherent in perturbative formalism, such as choice of infrared cutoff scales. However, the  $Q^2$  dependence of the transparency ratio is found to depend sensitively on the model of the distribution amplitude, with end-point-dominated models failing to be dominated by short distance. Color transparency experiments should provide an excellent test of the underlying theoretical assumptions used in the PQCD calculations.

PACS number(s): 13.40.Gp, 12.38.Bx, 14.20.Dh

### I. INTRODUCTION

Exclusive processes are an exciting frontier. However the applicability of perturbative QCD at the momenta currently accessible remains controversial. The quark-counting scaling laws of Brodsky and Farrar tend to agree remarkably well with data. This apparently indicates that a finite, minimal number of quarks is being probed. However, the helicity conservation selection rules of Brodsky and Lepage tend not to agree with data [1–3]. Failure of hadronic helicity conservation rules out dominance by the short distance formalism. Then the agreement of the scaling laws becomes rather mysterious. Theoretical criticisms focus on calculations found to include regions where the internal momentum transfers are too small for perturbative QCD (PQCD) to reliably apply [4,5]. For even the simplest model calculations, the case of hadronic form factors, it is found that large contributions come from the components of quark wave functions involving large quark spatial separations. This undermines restriction of the calculation to short-distance wave functions, which is nevertheless invariably done, causing problems with the theoretical consistency of the subject.

In contrast with exclusive processes in free space, it has been claimed [6–8] that the corresponding processes in a nuclear medium will be theoretically cleaner. Large quark separations will tend not to propagate in the strongly interacting nuclear medium. Configurations of small quark separations, on the other hand, which happen to be the perturbatively calculable region, will propagate with small attenuation. This phenomenon, called nuclear filtering [6–8], is the complement of the idea called color transparency

[9,10]. In its original rendition, color transparency [9,10] was based on having large momentum transfer  $Q^2$  select short distance, then free to propagate easily through a passive nuclear probe. Nuclear filtering uses the nuclear medium in an active way.

#### A. Filtering versus transparency

The distinction between nuclear filtering and color transparency is sharpened by considering different kinematic limits. For a given nucleus (nuclear number  $A$ ), the limit of  $Q^2$  going to infinity should show decreasing attenuation, and ultimately perfect “transparency” of a nucleus. The “transparency limit” of  $Q^2 \rightarrow \infty$  is unrealistic, however. The “filtering limit” takes  $A \gg 1$  with  $Q^2$  fixed and large enough to motivate a PQCD approach. In this case large  $A$  should eliminate many long distance amplitudes. On this basis, it has been predicted that calculations of exclusive reactions in PQCD are more reliable in a large nuclear target than in free-space.

These remarkable phenomena have some experimental support. Experimentally one finds that the fixed-angle free space process  $pp' \rightarrow p''p'''$  [11] shows significant oscillations at 90 degrees as a function of energy. The energy region of oscillations is not small, but extends over the whole range of high energy measurements that exist, from  $s = 6 \text{ GeV}^2$  to  $s = 40 \text{ GeV}^2$ . The oscillations are not a small effect, but fill out roughly 50% of the  $1/s^{10}$  behavior, and are interpreted as coming from interference of long and short distance amplitudes. The corresponding process in a nuclear environment  $pA \rightarrow p'p''(A-1)$  shows no oscillations, and obeys the PQCD scaling power law far better than the free-space data [6,12,8]. The  $A$  dependence, when analyzed at fixed  $Q^2$ , shows statistically significant evidence of reduced attenuation [13]. Note that 90 degrees is a special point, due to Fermi statistics, and that experimental study is needed at angles other than 90 degrees. One cannot conclude from a

\*Email address: bijoyk@iitk.ac.in

†Email address: jim@thep.lu.se

‡Email address: pkjain@iitk.ac.in

§Email address: ralston@KUHUB.PHSX.UKANS.EDU

single experiment that *all* long distance components have been completely filtered away, only that interference between large and small distance components is different inside the nucleus, and the long distance components are apparently reduced compared to in free space.

It is interesting, then, that other experiments appear to show the same phenomena. Data for the free space energy dependence of  $d\sigma/dt$  for  $\gamma p \rightarrow \pi^+ n$  and  $\pi p \rightarrow \pi' p'$  at fixed  $90^\circ$  c.m. angle shows oscillations quite like the oscillations seen in  $pp \rightarrow p' p''$ . The existence of this data has not been widely appreciated. Recent work [14] predicts filtering of the oscillation phenomena and two more cases of the transparency ratio oscillating with energy, which may be checked in the near future [15].

### B. Sudakov effects as vacuum filtering

It has long been known that the transverse separation of quarks in free space reactions is controlled by effects known as the Sudakov form factor. The Sudakov effect is closely related to nuclear filtering. It is somewhat novel, but fair, to observe that Sudakov effects are the filtering away of large transverse separations in the vacuum, enforced by the strict requirements of exclusive scattering. Li and Sterman [16] included Sudakov effects for the pion form factor, arguing that a perturbative treatment become fairly reliable at momenta of the order of 5 GeV. As low as 2 GeV, it was found that less than 50% of the contribution comes from the soft region. This countered earlier calculations, which argued that in free space close to 95% of the contribution to the form factor comes from the soft region [4,5]. The situation with the proton form factor is similar but has a larger theoretical uncertainty [17]. For example, the proper infrared cutoff to be imposed on the exponent in the Sudakov form factor has been controversial. Jakob et al. [18] argued that the cutoff used by Li [17] does not suppress all the end point singularities. By using a different infrared cutoff the magnitude of the form factor was shown to decrease. However, an improved and much more complete calculation [19] recently incorporated the full two loop correction to the Sudakov form factor. A very minor modification of the infrared cutoffs then finds good agreement with data. The remaining dependence on infrared cutoff implies that a significant contribution remains from a region of large distance.

### C. Computational approach

Previous calculations of color transparency phenomena have followed several dynamical approaches. In one approach, an initial state with size of order  $1/Q$  is postulated, which expands explosively as time evolution progresses. Different groups use different model dynamics: Farrar, Liu, Frankfurt and Strikman [20] model the process with simple classical physics. Blaizot [21] and Kopeliovich [22] model the time evolution with harmonic oscillator wave functions. Jennings and Miller [23] use complete sets in the hadronic basis, along with experimental matrix elements, to model the time evolution. Calculations within the different model dynamics schemes [8] show that the expansion rates depend strongly on model dynamics and the choice of initial states.

In contrast, we follow the PQCD approach. The impulse approximation for the hard scattering postulates a normal sized initial state [24]. While the struck state is full sized, one finds that only the short distance amplitudes dominate inside the integrations. The zero-distance wave functions are codified in the distribution amplitude formalism, upon which the short-distance Sudakov factors are built. The perturbative treatment in the impulse approximation includes ‘‘expansion’’ or diffusion in the quantum mechanical propagation of quarks sideways and longitudinally [25,26]. We will discuss this in detail below. We will use an eikonal form [27] consistent with PQCD for the effects of interaction with the nuclear medium.

While primarily made for concept exploration, our calculations include all effects needed for comparison with data, except for important fine-tuning of kinematics to match details of experimental observations. Such details vary from experiment to experiment: in their absence, we have chosen an idealized kinematic point of zero momentum transfer to the nucleus. By explicit calculation, this point has been found to differ with a calculation involving realistic experimental resolutions to within less than 10%. When experimental kinematics become available we can include them. Surprisingly, we find that the main uncertainty in the nuclear calculation arises from uncertainties in the nuclear medium itself. In particular, uncertainties in the nuclear spectral functions and correlations are sizable. With standard assumptions one can proceed with the calculation essentially using zero parameters and no model dependence. However, we find that numerical differences between models of nuclear matter are large enough to cause significant uncertainties. Indeed, comparison with data shows that the uncertainties in the nuclear spectral functions and the nuclear correlations now dominate the theoretical uncertainties, and are larger effects than, for example, the dependence on the choice of infrared cutoff scale. This is surprising progress.

The paper is organized by presenting the kinematic framework for electroproduction of pion targets from a nuclear medium in some detail. This is followed by the more complicated calculation for nucleon targets. A separate section gives results and brief comparison with data.

## II. $\gamma^* \pi$ SCATTERING IN A NUCLEAR MEDIUM

We briefly review the framework for calculation of hadronic form factors following Li and Sterman [16]. We first consider the case of pion.

Let  $P$  and  $P'$  be the incident and outgoing momenta of the hadrons scattered by the  $\gamma^*$ . From factorization the diagrams are grouped into 3 kinds: the power-behaved hard scattering kernel, the resummed soft and collinear regions responsible for logarithmic evolution and Sudakov effects, and the non-perturbative wave functions. In the impulse approximation we integrate over the respective ‘‘minus’’ momenta of partons moving fast in the proper ‘‘plus’’ direction along  $P$  or  $P'$ . [Our convention is  $k^\pm = (k^0 \pm k^3)/\sqrt{2}$ .] The conjugate variable  $x^+$  is the light cone time variable of the partons, evaluated at zero, setting up the impulse approximation. The longitudinal + momentum fractions are denoted by

the Feynman variable  $x_i$  for the  $i$ -th parton. We let  $b_{ij}$  be the transverse separation between quarks  $i$  and  $j$ , or  $b$  the corresponding quantity for a single pair of quarks.

In the Brodsky-Lepage formalism,  $Q^2 \rightarrow \infty$  is taken at the first step. The result is that  $b$  is set to zero, leaving convolutions of a hard scattering kernel and distribution amplitudes that depend only on  $x$  and  $Q^2$ . The innovation of Li and Sterman includes the Sudakov form factor dependence on  $b$  inside the integrations, and afterwards takes the limit of large  $Q^2$ . Including the  $b$  dependence, the pion electromagnetic form factor can be written as

$$F_\pi(Q^2) = \int dx_1 dx_2 \frac{d\vec{b}}{(2\pi)^2} \mathcal{P}(x_2, \vec{b}, P', \mu) T_H(x_1, x_2, \vec{b}, Q, \mu) \times \mathcal{P}(x_1, \vec{b}, P, \mu). \quad (1)$$

Here

$$\mathcal{P}(x, b, P, \mu) = \exp(-S) \phi(x, 1/b) + O(\alpha_s(1/b)),$$

plays the role of the hadron wave functions, where  $\phi(x, 1/b)$  is the meson distribution amplitude.  $T_H(x_1, x_2, \vec{b}, Q, \mu)$  is the hard scattering kernel, which after incorporating the renormalization group (RG) evolution from the renormalization scale  $\mu$  to  $t$ ,  $t = \max(\sqrt{x_1 x_2} Q, 1/b)$ , is given by [16]

$$T_H(x_1, x_2, \vec{b}, Q, \mu) = \exp\left[-4 \int_\mu^t \frac{d\bar{\mu}}{\bar{\mu}} \gamma_q(\alpha_s(\bar{\mu}))\right] \times T_H(x_1, x_2, \vec{b}, Q, t). \quad (2)$$

$S$  is the Sudakov form factor:

$$S(x_1, x_2, b, Q) = \sum_{i=1}^2 [s(x_i, b, Q) + s(1-x_i, b, Q)] - 4 \int_\omega^t \frac{d\bar{\mu}}{\bar{\mu}} \gamma_q(\alpha_s(\bar{\mu})). \quad (3)$$

$\gamma_q(\alpha_s)$  in the above equations is the quark anomalous dimension. Our symbols are the same as used by Li and Sterman [16], who give explicit formulas for  $T_H, s(x_i, b, Q), \gamma_q$  and so on. The improved factorization used in [16] retains the intrinsic transverse momentum  $k_T$  dependence in gluon propagators, since  $k_T$  need not be small compared to  $\sqrt{x_1 x_2} Q$ . In particular there is a dangerous region if any of the  $x_i$  get close to zero. The variable  $b$  in Eq. (1) is conjugate to  $k_{T1} - k_{T2}$ , where  $k_{T1}$  and  $k_{T2}$  are the transverse momenta of the incident and outgoing partons. As long as  $x_1$  and  $x_2$  are not close to their endpoints, the dominant scale in the scattering is  $\sqrt{x_1 x_2} Q$  and the small  $b$  region dominates the amplitude. Close to the end points,  $\sqrt{x_1 x_2} Q$  may become small. However, the large  $b$  region is strongly damped by the Sudakov form factor. The results for the free space form factor for the pion using this procedure are given in [16]. The authors show that at  $Q^2 = 5 \text{ GeV}^2$ , something like 90% of

the contribution comes from a region where  $\alpha_s/\pi$  is less than 0.7 and hence could be regarded as perturbative.

### A. The pion: nuclear medium effects

The nuclear medium modifies the quark wave function such that [7]

$$\mathcal{P}_A(x, b, P, \mu) = f_A(b; B, z) \mathcal{P}(x, b, P, \mu), \quad (4)$$

where  $\mathcal{P}_A$  is the wave function inside the medium and  $f_A$  is the nuclear filtering amplitude. The formalism predates Li and Sterman, and naturally has the same kinematic dependence (modification of the  $b$ -space wave function) due to the parallel between nuclear filtering and vacuum filtering by Sudakov resummation. An eikonal form [27,28] is appropriate for  $f_A$ :

$$f_A(b; B, z) = \exp\left(-\int_z^\infty dz' \sigma(b) \rho(B, z')/2\right). \quad (5)$$

Here  $\rho(B, z')$  is the nuclear number density at longitudinal distance  $z'$  and impact parameter  $B$  relative to the nuclear center. We have used the fact that the imaginary part of the eikonal amplitude for forward scattering is related to the total cross section, explaining our use of the symbol  $\sigma(b)/2$ . Finally, we must include the probability to find a pion at position  $B, z$  inside the nucleus, which we take to be a constant times the probability to find a nucleon. Putting together the factors, the transparency ratio  $T$  is calculated from

$$T = \frac{d\sigma_{\text{nuclear}}}{A d\sigma_{\text{free space}}},$$

where  $A$  is the nuclear number. Some theory groups prefer division by a model calculation, which introduces a potential model dependence of the definition, explaining why we use the original definition of Carroll et al. [11]. The nuclear cross section is calculated by incoherently adding the contribution due to individual nucleons.

The inelastic cross section  $\sigma$  is known to scale like  $b^2$  as  $b \rightarrow 0$  in PQCD [29,30]. We parametrize  $\sigma(b)$  as  $k b^2$  and adjust the value of  $k$  to find a reasonable fit to the experimental data. Introduction of this parameter might be avoided. There is a long history of relating cross sections to diffractive calculations of the same kind in PQCD. For reasons to be explained below, we retain the parameter here.

### B. Important details

Let us comment on some important details of the calculation.

*Nuclear densities.* Nucleon number densities were taken from Atomic Data and Nuclear Data Tables [31]. The pion case uses straight densities as quoted and then proton case (discussed below) includes nuclear correlations in the form of an effective density distribution.

*Wave functions.* For the  $x$ -dependence of wave functions we used the Chernyak-Zhitnitsky (CZ) and asymptotic distribution amplitudes. We chose not to complicate the calcu-

lation with models of the soft  $b$ -space dependence. These can be inserted as necessary: by leaving out such factors, one can more easily see from inspection the relative effects of Sudakov and nuclear filtering.

*Experimental momentum resolution.* In nuclear calculation we have integrated over the transverse impact parameter  $B$  and longitudinal coordinate  $z$  locating the targets in the nucleus. From translational invariance, the coherent superposition over the nucleus with net momentum transfer  $\vec{K}$  includes a phase  $\exp(-iB_T K_T - iK_z z)$ . The phase is not indicated because we set  $\vec{K}=0$  for the numerical calculations presented in Sec. III. However, we also repeated the calculations for finite  $\vec{K}$  to check the dependence on this. In the region of  $K_T, K_z$  ranging from  $-25$  MeV to  $25$  MeV, the results for the Au=197 nucleus changed by less than 10%: specifically decreasing by a maximum of 7.7% for the pion and 8.3% for the proton. For rigorous comparison with experiments one would want to include the effects of finite  $\vec{K}$  integrated over the same range as experimentally observed. The treatment of Fermi momentum is of course related, and should be matched consistently whenever models are used for experimental extraction.

*Experimental subprocess identification.* The experimental extraction of the pion form factor in free space assumes certain kinematic criteria are imposed. A  $t$ -channel singularity, and consistency with the angular distribution of the spin-zero form factor are part of proper ‘‘Rosenbluth separation’’ extracting the form factor [32]. Experimental cuts determine whether other subprocesses not involving the form factor [33] can contribute to the observables, leading to a well-defined procedure. We assume equivalent criteria are applied to the experimental study of knocking a pion out of the nucleus, and note that this is compatible with the momentum transfer  $\vec{K}$  discussed above. With use of over-determined kinematics such as the BNL experiment has demonstrated, the identification of this quasi-elastic subprocess seems quite feasible.

### C. Expansion

A controversial element of color transparency and nuclear filtering is the topic of ‘‘expansion.’’ The term describes the time evolution of the struck system as it moves through the nucleus. Some calculations model this using a hadronic basis assumed to be a complete set. Experience from nuclear physics calculations are then brought to the problem. On the other hand, the foundations are unclear, because many phenomena involving quarks, including such basic features as scaling in inclusive reactions, defy successful description in a hadronic basis. The transformation between the fundamental quark basis in which transparency has been predicted, and the hadronic basis of model calculations, cannot be explicitly written down. Due to this clash there has been a great deal of confusion.

Perturbative calculations in the quark basis naturally include time evolution. The basic element in perturbation theory is the Feynman propagator,  $1/p^2 + i\epsilon$ , for a free particle of momentum  $p$ . The imaginary part is  $i\pi\delta(p^2 - m^2)$ .

We transform this partly to coordinate space to see the time-evolution  $U(b, x^+; p^+)$  in light cone time  $x^+$  and transverse coordinate  $b$ , obtaining

$$U(b, x^+; p^+) \approx \frac{1}{p^+} \exp(-ib^2 p^+ / 2x^+ + im^2 x^+ / 2p^+).$$

This has been called ‘‘quantum diffusion,’’ but it represents nothing more than propagation of a free, relativistic particle from a point source. Ordinary perturbation theory includes this expansion (and much more) in the convolution of Green functions over all points linked in the Feynman diagrams: the series of integrals of  $\Delta_F(x^\mu - x'^\mu) \Delta_F(x'^\mu - x''^\mu) \dots$ , somewhat concealed when calculations are done in momentum space.

The question of expansion, then, is how much physical expansion is reproduced by the propagation implemented by perturbation theory. In coordinate-space the integration regions include light-like displacements much larger than the nuclear size and extending over the entire volume of transverse separation possible. Whatever the idealizations of factorization arguments, the actual calculations include both far off-shell regions from the scattering kernel associated with short-distance propagation, and nearly on-shell regions evolving with proper perturbative quantum mechanical expansion over long-distances. The system interacts with the nucleus over the entire process, as the  $x, b, B, z$  integrals are totally coupled without any separation: Thus, sideways propagation is linked to the  $z$  propagation. This fact has been misunderstood, perhaps due to attention to the *asymptotic* limit in which this same formalism has been able to establish that the effects of the nucleus are decoupled [7].

Unfortunately we do not know how to translate the regions of integration of the quark variables into the hadronic basis. Given a perfect ‘‘rosetta stone’’ we could predict exactly what hadronic picture applies, and which details of the hadronic spectrum such as the masses and widths of resonances are already included, or need to be added. The situation is exactly like the mystery of duality noticed by Bloom and Gilman [34] in deeply-inelastic scattering. Twenty years later, there has been little progress in explaining how a simple perturbative quark-picture prediction of structure functions manages to interpolate precisely between resonances and successive thresholds of daunting complexity in the hadronic basis. On this basis, quark perturbation theory definitely reproduce multiparticle continuum hadronic states in the time-evolution with some reliability. However, on the same basis, PQCD does not pretend to reproduce detailed structure at particular momenta due to resonances. From this we believe that the expansion occurring in our calculations is of the nature of a multi-state average when viewed in the hadronic basis. It is expansion of one kind, which would not include fine details of particular resonant mixing of states. It is an open question whether details of the hadronic spectrum matter in the problem: the problem is closely related to determining the precise kinematic region where PQCD would apply.

**D. Central versus endpoint wave function models**

The calculations we report depend on the models of the distribution amplitudes. For discussion we can classify models as ‘‘end-point’’ or ‘‘centrally’’ dominated, with typical endpoint models being those of QCD sum rules [3,35], and typical central models being the asymptotic distribution amplitude [2]. Experience in free space form-factor calculations teaches us that endpoint models tend to be contaminated by long distance contributions while central models tend to be more dominated by short distance. Comparison of experimental data with the pion form factor is fairly inconclusive and does not favor either class of models [32]. If one allows for some reasonable variations within the classes, for example not really believing the normalizations of the QCD sum rule predictions, then the ambiguity becomes even worse. Given this situation, we made calculations using representatives from both classes, and without assuming too much is known about the normalization of the distribution amplitudes. We then compare the calculations to see what each type of model predicts.

**E. Discussion**

Elsewhere we have emphasized that quasi-exclusive pion scattering in a nuclear medium should be very interesting to measure [25,26]. While the pion’s small mass makes large momentum transfers more difficult, there are reasons to believe that experiments at accessible momentum transfers should be pursued.

First, calculations of meson form factors are comparatively reliable: They are certainly much better than baryon form factors. The pion is uncomplicated compared to the proton, lacking the infamous ‘‘double -flow’’ configuration [36]. The pion also allows fewer covariant wave functions that could allow orbital angular momentum to flow. Pion decay directly measures a short distance wave function normalization, pinning down another variable. Finally, the short-distance prediction for the pion electromagnetic form factor is apparently not far from the data in free space.

The upshot is that short distance concepts ‘‘almost work’’ for the pion in free space, and theory is easier. When one does not have to rely much on nuclear filtering, it becomes a good approximation to consider the calculation inside the nuclear target as a free-space form factor followed by some propagation. In that approximation one does not need to know the form factor, which is argued to cancel out in ratios to free-space processes. (Indeed, much of the theory literature is locked into the approximation that the form factor cancels out, because only propagation is calculated.) Under those ideal conditions, the transparency ratio as a function of  $Q^2$  serves its naive function of measuring transparency.

The general situation cannot be so simple. The instant one acknowledges that the short distance component inside the nuclear target is not the same as in free space, then the normalization of the hard scattering is changed [13]. The effect is not small when current calculations put 50% of the amplitude as ‘‘soft’’: One cannot then consistently argue that some universal form factor ‘‘cancels out’’ in a naive ratio. Fortunately one can also study the  $A$  dependence at fixed  $Q^2$  and

convert this uncertainty into productive measurements of attenuation. This is discussed in Sec. IV.

On the other hand, the effects from uncertainties in nuclear parameters are about the same for a pion or proton target. These uncertainties also do not cancel out in ratios, do not disappear with increasing  $Q^2$ , and are not much ameliorated by large  $A$ . At the moment we simply have to live with these uncertainties.

**III.  $\gamma^*$ -NUCLEON SCATTERING IN A NUCLEAR MEDIUM**

The calculation of the proton form factor [17] in free-space is rather more complicated than for the pion. Underlying the difficulty is that there are two quark transverse separation scales, each of which must be controlled by Sudakov and nuclear filtering.

The factored decomposition for the proton form factor derived in [17] is similar to that for the pion but much more complicated. Our notation follows Ref. [17] which define the symbols with lengthy expressions we need not repeat in detail here. All wave function terms are gathered together in a symbol  $\Psi_j$ . The hard scattering kernels are gathered together in a symbol  $\tilde{H}_j$ . There are altogether 48 separate Feynman diagrams to be summed over, but (as shown by Li [17]) symmetries of indices related by permutations reduce the sum over  $j$  to two terms,  $\tilde{H}_1, \tilde{H}_2$ . The permutations require introduction of symbols  $t_{11}, t_{21}$  and  $t_{12}$ , which are notations for scales that are the larger of  $1/b_i, x_i Q$ . Internal quark light cone fractions are denoted by  $x$ , and transverse separations by  $b_1, b_2$ . There are  $4x$  integrations,  $2b$  integrations, and one relative angle integration  $\theta$  to calculate the form factor:

$$\begin{aligned}
 F_1^p(Q^2) = & \sum_{j=1}^2 \frac{4\pi}{27} \int_0^1 (dx)(dx') \\
 & \times \int_0^\infty b_1 db_1 b_2 db_2 \int_0^{2\pi} d\theta [f_N(cw)]^2 \\
 & \times \tilde{H}_j(x_i, x'_i, b_i, Q, t_{j1}, t_{j2}) \Psi_j(x_i, x'_i, cw) \\
 & \times \exp[-S(x_i, x'_i, cw, Q, t_{j1}, t_{j2})], \tag{6}
 \end{aligned}$$

with

$$(dx) = dx_1 dx_2 dx_3 \delta\left(\sum_{i=1}^3 x_i - 1\right).$$

Here  $f_N$  is the proton normalization constant and  $cw$  play the role of factorization scale, above which QCD corrections give the perturbative evolution of the wave function  $\Psi_j$  in Eq. (6), and below which QCD corrections are absorbed into the model distribution amplitude  $\phi$ .

The Sudakov exponent  $S$  is given by

$$\begin{aligned} S(x_i, x'_i, cw, Q, t_{j1}, t_{j2}) &= \sum_{i=1}^3 s(x_i, cw, Q) + 3 \int_{cw}^{t_{j1}} \frac{d\bar{\mu}}{\bar{\mu}} \gamma_q(\alpha_s(\bar{\mu})) \\ &+ \sum_{i=1}^3 s(x'_i, cw, Q) + 3 \int_{cw}^{t_{j2}} \frac{d\bar{\mu}}{\bar{\mu}} \gamma_q(\alpha_s(\bar{\mu})). \end{aligned} \quad (7)$$

Here  $s(x_i, cw, Q)$  is called the Sudakov function and its explicit expression is given in [16], while  $\gamma_q$  is an anomalous dimension. We have shown the Sudakov form factor to emphasize explicitly that the region of large  $b$ , or regions of  $x \rightarrow 0, x \rightarrow 1$  is suppressed as  $Q \rightarrow \infty$ .

### The proton: nuclear medium effects

For the proton we use the same procedure for effects of the nuclear medium as used for the pion except that now we use the inverse of the factorization scale  $cw$  to calculate the attenuation cross section of proton inside the nucleus. Here  $1/w$  is taken to be the maximum of the three distances in a proton i.e.  $1/w = b_{\max} = \max(b_1, b_2, b_3)$ . We again set  $\vec{K} = 0$  for our calculations as used for the pion, as the effects of finite  $\vec{K}$  are less than 10%. Overall, then, the calculation of the process in the nuclear target needs a 9 dimensional integration, which is performed by the Monte Carlo method. Results are presented in Sec. IV. We now turn to specifying important details.

### Calculational details

*Wave functions and infrared cutoffs.* As in the pion case, the calculations for the proton free-space and nuclear filtered processes depend on the model of the distribution amplitudes. End-point models tend to greatly exacerbate the problem of long distance contributions: at the same time these models tend to be the ones used to fit data for the proton form factor. We will report calculations with both the CZ [3] and King-Sachrajda (KS) [35] end point models, and also a central model, and then compare them.

There has been some controversy regarding the proper choice of the infrared cutoff in the Sudakov exponent. The factorization scale  $cw$  separates the perturbative and the non-perturbative contributions in the wave function  $\mathcal{P}$ . The choice  $c=1$  proposed in [18] uses the largest distance between the three quarks as the cutoff. It was found that this choice gave results about 50% smaller than the experimental data for the form factor. One can argue that the result may be reasonable, if other wave functions (and in particular, non-zero quark angular momentum) contribute heavily in free space. On the other hand, in Ref. [19] it was observed that the largest distance does not correspond to a physical size of the three quark system. A more appropriate infrared cutoff might consider a configuration of the quark-diquark type. The resulting cutoff value  $c=1.14$  uses the maximum distance between quark and diquark. Remarkably, this small modification with the KS distribution amplitude leads to results in good agreement with the experiment [19].

Agreement with experiment can be good, but one can play devil's advocate, and argue that if various contributions at the 50% level exist, perhaps the short distance distribution amplitudes currently in vogue are not properly normalized, but are effectively renormalized to arrange agreement with data. The issue cannot be resolved because different contributions with different signs may cancel. In our calculations we chose the infrared cutoff parameter  $c=1.14$ .

*Nuclear correlations.* Following the procedure of Lee and Miller [37], the effects of short-range correlations were included approximately by the replacement

$$\rho(B, z') \rightarrow \rho(B, z') C(|z - z'|), \quad (8)$$

where  $\rho(B, z')$  is the nuclear density at the longitudinal position  $z'$  and impact parameter  $B$  relative to the nuclear center and  $z$  is the longitudinal position of the point of hard collision.  $C(u)$  is a correlation function estimated in [38] to be  $C(u) = [g(u)]^{1/2}$  with

$$g(u) = \left[ 1 - \frac{h(u)^2}{4} \right] [1 + f(u)]^2 \quad (9)$$

where

$$h(u) = 3 \frac{j_1(k_F u)}{k_F u}, \quad (10)$$

$$f(u) = -e^{-\alpha u^2} (1 - \beta u^2) \quad (11)$$

with  $\alpha = 1.1$ ,  $\beta = 0.68 \text{ fm}^{-2}$  and the Fermi momentum  $k_F = 1.36 \text{ fm}^{-1}$ .

## IV. RESULTS AND DISCUSSIONS

Experimental results have been reported as a ‘‘transparency ratio’’ between cross sections. Such ratios depend strongly on what one chooses in the denominator. For the purpose of reporting our calculations we have divided our cross sections by  $A$  times the cross section from a free proton which was also the choice adopted by the BNL experiment [11]. Thus our transparency ratio ‘‘T’’ is the ratio of the square of a form factor with  $F_1$  Dirac structure for the nuclear target divided by  $F_1^2(Q^2)$ . As mentioned earlier, details of kinematic acceptance and assumed nuclear spectral distribution are needed for precise comparison with data.

### A. The pion

In Fig. 1 we show the  $Q^2$  dependence of the transparency ratio for electroproduction of pions using two different distribution amplitudes, the CZ and central forms. The scale of  $Q^2$  ranging up to  $5 \text{ GeV}^2$  may benefit from explanation. At the exclusive production point, the relativistic boost factor of a pion is given by  $\gamma = Q^2 / (2m_\pi^2) \sim 25(Q^2 / \text{GeV}^2)$ . Since even a 1 GeV pion is highly relativistic, we may suppose that the perturbative calculations may well apply in the comparatively small  $Q^2$  regime. These calculations show a rather striking rise with  $Q^2$  of the transparency ratio, which should

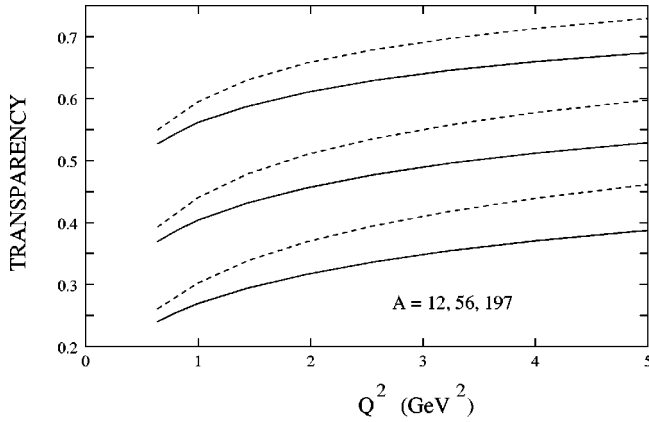


FIG. 1. The calculated pion transparency ratio for different nuclei as a function of  $Q^2$ . The solid and dashed curves use the CZ and asymptotic distribution amplitudes respectively and correspond to  $A = 12, 56$  and  $197$  from top to bottom.

be easily observable experimentally. The fact of the rise does not depend much on the distribution amplitude, but the *slope* of the rise does: we discuss the reasons in the section discussing the proton. For these calculations we used  $\Lambda_{QCD} = 200$  MeV. We adjusted the value of  $k$  so that the predicted results for proton (discussed later) are in agreement with the SLAC data [39,40]. This selects the value of  $k$  to be 10. This value was determined self-consistently. Its coincidence with the parameter chosen for the pion indicates consistency between the two calculations. Of course, after the integrations are done, different regions contribute and the proton tends to have larger cross sections than the pion. More precise values of  $k$  might be obtained after making a fit to data, or perhaps with more detailed comparison with diffractive calculations.

Figure 2 shows the  $A$  dependence of the pion transparency ratio at fixed  $Q^2$ . The curvature of the  $A$  dependence at fixed  $Q^2$  is a way to extract the effective attenuation cross section independent of the normalization of the initial state. The normalization of the ratio is an entirely different affair, which drops out of the extraction of attenuation cross sections.

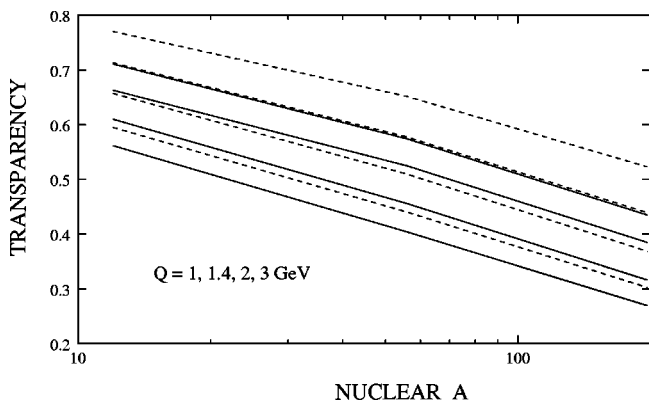


FIG. 2. The calculated pion transparency ratio as a function of nuclear  $A$  for different  $Q$ . The solid and dashed curves use the CZ and asymptotic distribution amplitudes respectively and correspond to  $Q = 1, 1.4, 2$  and  $3$  GeV from bottom to top.

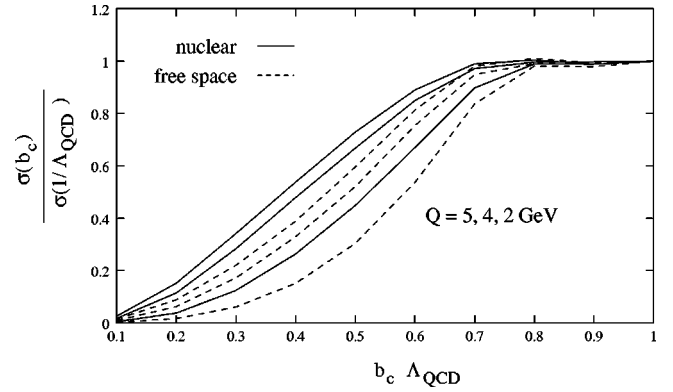


FIG. 3. The transverse separation cutoff  $b_c$  dependence of the pion cross section in the nuclear medium (solid curve) and free space (dashed curve). The quantity  $\sigma(b_c)$  is a cutoff dependent reduced cross section calculated by putting a cut  $b_c$  on the transverse separation between the two quarks. The results have been normalized to unity as  $b_c$  approaches its maximum value  $1/\Lambda_{QCD}$ . The three different curves in each case, left to right, correspond to  $Q = 5, 4$  and  $2$  GeV, respectively. Calculations are for  $A = 197$ .

The pion calculation is quite transparent, that is, one can easily see the large transverse separation region being reduced by nuclear filtering. To quantify this, we introduce a working concept of the *cutoff dependent cross section*, which we define to be the scattering cross section calculated by imposing a cutoff on the quark transverse separation parameter  $b$ . This terminology should not cause confusion and serves a purpose for quick visual inspection of  $Q^2$  and cut-off dependence. In Fig. 3, we show the cutoff  $b_c$  dependence of the pion scattering cross section ratio. In an ideal short-distance dominated problem, the cut-off dependence would be absent, and 100% of the amplitude would occur after integrating up to  $b_c$  of order  $1/Q^2$ . Cut-off dependence persists, but compared to free space the nuclear medium significantly attenuates the large distance contribution. Thus PQCD is more reliable in the nuclear calculation.

### B. Extracting the effective attenuation $\sigma_{eff}$

Finally, we have extracted the effective attenuation cross section  $\sigma_{eff}(Q^2)$ , which serve as a litmus test of whether “color transparency” has actually been achieved.

If one knew for sure that the hard scattering were a short-distance process, then this procedure would be a complementary test. However, when the hard scattering cannot be claimed to “divide out” of the process at realistic  $Q^2$ , then attenuation becomes central and should really be extracted. Following Ref. [13] we define  $\sigma_{eff}(Q^2)$  by fitting the curvature of the  $A$  dependence of the transparency ratio at fixed  $Q^2$ . In the process, we let a ( $Q^2$  dependent) normalization float. This process eliminates uncertainties caused by division by a poorly understood free space process: one can divide by anything fixed, or simply use the cross section in the nuclear target without division.

The results (Fig. 4) show a significant decrease of  $\sigma_{eff}(Q^2)$  with increasing  $Q^2$  to values well below the Glauber model attenuation cross section. The calculations

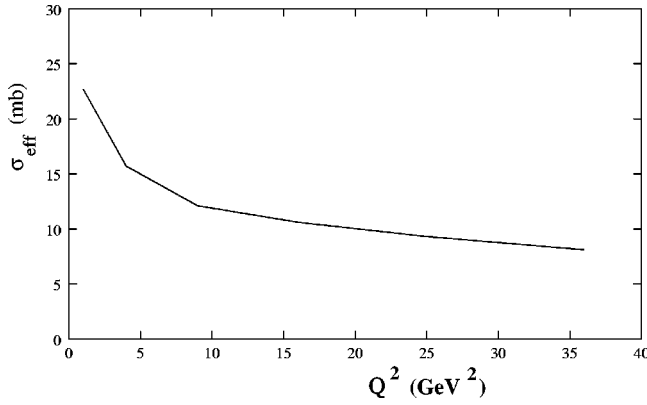


FIG. 4. Extracted pion effective attenuation cross sections  $\sigma_{\text{eff}}(Q^2)$  as a function of  $Q^2$  exhibit color transparency. The calculations fit the curvature of the  $A$  dependence in terms of two parameters  $N$  and  $\sigma_{\text{eff}}$  for each  $Q^2$ , where  $N$  is the overall normalization of hard scattering in nuclear medium and  $\sigma$  measures the nuclear attenuation [13]. The decrease of  $\sigma_{\text{eff}}(Q^2)$  with  $Q^2$  indicates that PQCD predicts very significant color transparency effect for the case of pion. The CZ distribution amplitude has been employed for these calculations.

were made in the CZ model; the asymptotic case is similar. We found that the normalization ranges from 0.88 to 0.94 as  $Q^2$  varies between 1 GeV<sup>2</sup> to 36 GeV<sup>2</sup>. We therefore find that the  $\sigma_{\text{eff}}(Q^2)$  which best describes the process is smaller than what would have been obtained if the normalization were arbitrarily set equal to unity. Thus the difficulty anticipated on the basis of data some years ago [13] has turned out to be a proven feature of the calculations.

The potential scientific value of measuring  $\sigma_{\text{eff}}(Q^2)$  is very great. The quantity has the power to rule out conventional nuclear physics, independent of rapid  $Q^2$  dependence, and confirm color transparency.

### C. The proton

In our calculations the parameter  $k$  in the attenuation cross section  $\sigma = kb^2$  was chosen so as to provide a reasonable fit

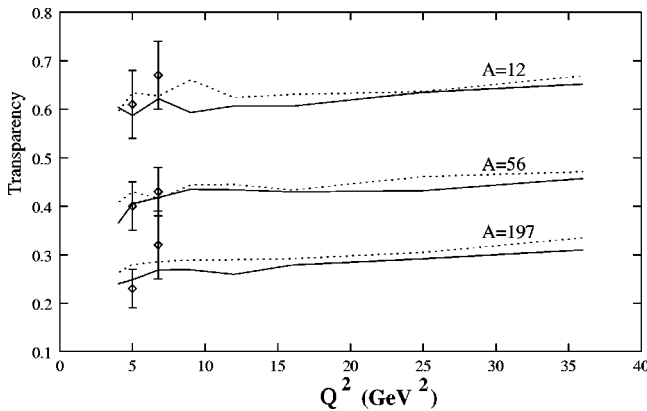


FIG. 5. The calculated transparency ratio for the proton for different nuclei using the KS endpoint dominated model for distribution amplitude. The experimental points are taken from Refs. [26,27]. The solid curves are calculated with  $k=10$  and the dashed curves with  $k=9$ .

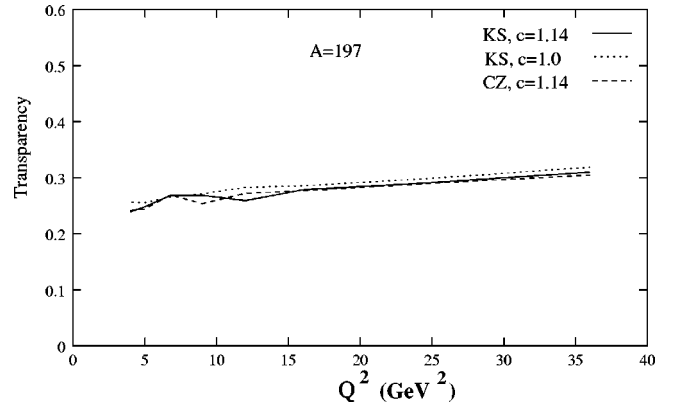


FIG. 6. The sensitivity of the calculated transparency ratio to different proton distribution amplitudes and the factorization scale parameter  $c$ . The solid, dotted and dashed curves correspond to the KS wave function with  $c=1.14$ , KS distribution amplitude with  $c=1.0$  and the CZ distribution amplitude with  $c=1.14$  respectively. All calculations use  $A=197$ .

to the experimental data [39,40]. We find that a value of  $k=10$  gives a reasonable fit. Since the data for  $T$  is available only in the region where the calculated free space form factor is in disagreement with the experimental result, the values of  $k$  obtained by this procedure cannot be taken too seriously. In fact, parameter  $k$  would be best obtained by fitting to the experimental value of  $T$  after it is measured at higher energies. A reasonable range of  $k$  values, which we take to be  $k=9$  and  $k=10$  has been used in the figures. We note parenthetically that the extrapolation of the short-distance  $\sigma = kb^2$  rule into the regime of large  $b$  might be modified to explore other models. We did not pursue that here, in order to report clearly defined calculations, perturbatively driven and perturbatively consistent.

Results for the  $Q^2$  dependence of the proton transparency ratio from various models are shown in Figs. 5, 6, and 7. The nuclear  $A$  dependence is shown in Fig. 8. A standard model for the distribution amplitude, the KS model, was used to generate Fig. 5. One sees that the calculation with the KS model has a rather flat  $Q^2$  dependence. At first this result was surprising, assuming a short-distance picture and a rapidly

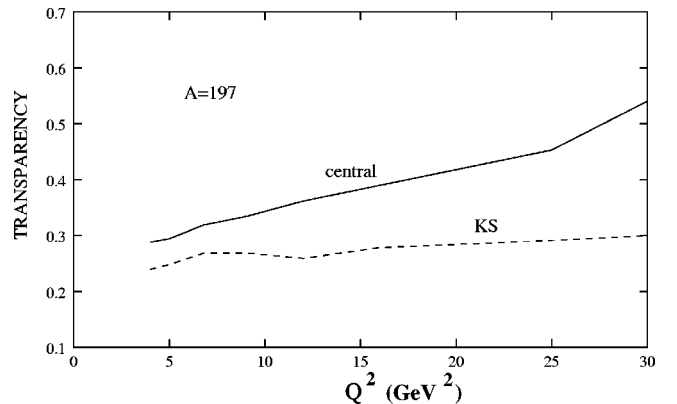


FIG. 7. The calculated transparency ratio using a central model distribution amplitude for  $A=197$ . The result using KS distribution amplitude is shown for comparison

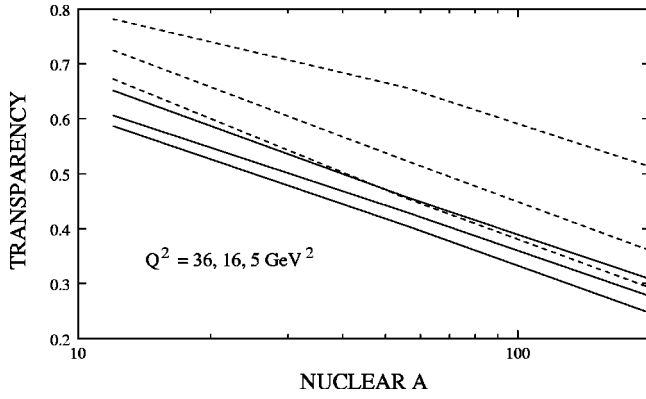


FIG. 8. The  $A$  dependence of the transparency ratio for different values of  $Q^2 = 36, 16, 5 \text{ GeV}^2$  (top to bottom), calculated in the KS end-point-dominated model (solid lines) and a centrally peaked model (dashed lines) with  $k = 10$ . The parallelism of the lines in the KS model illustrates next to no change in curvature of the  $A$  dependence, consistent with little observable signs of short-distance in this model.

increasing function of  $Q^2$ , but in retrospect the result appears quite natural. As in the earlier discussion of the pion, our results depend on the distribution amplitude model, which can be categorized into two types. The KS model is an *end-point*-dominated distribution amplitude, which is known to produce its dominant contributions from long-distance components of the quark wave functions. For this reason use of the KS wave function in the free-space form factor has led to many questions of theoretical consistency, which we need not resolve here in this exploratory study. It is precisely the lack of a substantial short-distance contribution which is seen in our calculations to be responsible for the calculated flat dependence on  $Q^2$ . Turning to Fig. 6, which compares the CZ and KS models, both of which are endpoint dominated, one sees nearly identical flat  $Q^2$  behavior. This indicates that the details of the model do not matter so long as they are endpoint models. The figure also shows the dependence on the infrared parameter  $c$ . Rather interestingly, a substantial dependence on  $c$  of form factors in free space drops out in the transparency ratio.

As pointed out by Abbott *et al.* [41], systematic errors in the transparency ratio due to the uncertainty in the nuclear spectral functions are of the order of 4% for C to 11% for Au. If one assumes an endpoint distribution amplitude of the type currently in use, we find that these uncertainties in nuclear modeling currently dominate the error in the calculation.

The  $Q^2$  dependence of transparency ratio, shown in Fig. 5, shows structure with “bumps,” whose origin appears to be numerical errors in the Monte Carlo integration. The error in the free space and nuclear cross section calculation is about 3% and 4% respectively. As the accuracy of the integration is increased, the amplitude of the bumps tends to decrease. In many cases the bumps also are found to randomly shift to different values of  $Q^2$  and hence are consistent with random fluctuations. Nevertheless the remote possibility that bumps might exist in the transparency ratio and be experimentally observable cannot be dismissed.

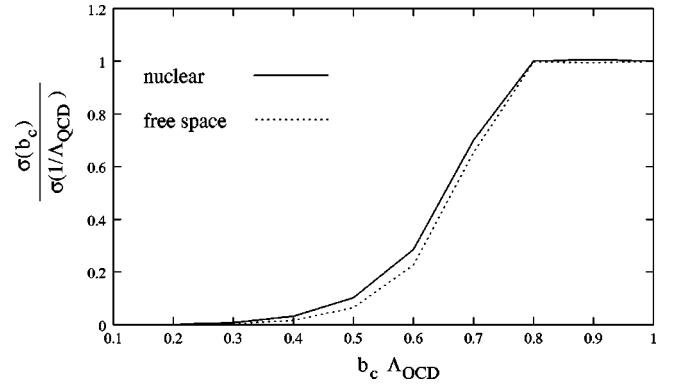


FIG. 9. Dependence on transverse separation cutoff  $b_c$  for  $A=197$  and  $Q^2=36 \text{ GeV}^2$ . The quantity  $\sigma(b_c)$  is a cutoff dependent reduced cross section calculated by putting a cut  $b_c$  on the transverse separation between the quarks. The results have been normalized to the value at the maximum possible  $b_c = 1/\Lambda_{QCD}$ . These calculations, in the KS end-point-dominated model, show little dominance of short distance consistent with the flat transparency dependence with  $Q^2$  of the same model.

#### D. Long versus short distance

Evidence of dominance by the long distance contributions in the endpoint models is shown in Fig. 9, the dependence on a transverse separation cutoff  $b_c$ . The plot was generated by integrating the largest quark separation from zero to an upper limit given by  $b_c$ , and then normalizing the result to the value at the maximum  $b_c = 1/\Lambda_{QCD}$ . Even with the filtering effects of the nucleus, there is very little saturation and very little difference between the nuclear and free-space cases. From Fig. 9 we see that the dominant contribution arises from a very narrow range of  $b$ . This appears to be the main reason why we see greatly reduced filtering effects in the proton compared to the pion. Numerical experiments showed that by adjusting  $k$  arbitrarily, we could force substantially more filtering, and a higher proportion of short-distance contribution in the end-point models. However we were unable to make such adjustments realistically while maintaining reasonable absorption cross sections, and therefore abandoned the attempt to make the KS model into a short-distance one. We also note that we can enhance the short distance contribution in any model by lowering the value of the infrared cutoff parameter  $c$ . Reducing  $c$  essentially forces the Sudakov exponent to cut off the integrals at a smaller value of  $b$ . An enhancement in filtering follows, which is expected since the integral becomes less dominated by the region  $b \approx 1/\Lambda_{QCD}$ .

Many other wave functions can be conceived: We wholeheartedly believe that the wave functions are unknown and that attempts to validate the CZ or KS models with data from free-space are rather questionable. To explore the effects we took a model which is highly central, a distribution amplitude with the structure

$$P(x_i) = x_1 x_2 x_3.$$

In this context we ignored  $QCD$  sum-rule lore about the normalization of various wave functions and simply postu-

lated a typical central wave function. The coincidence between this model and the asymptotic one derived by Brodsky and Lepage is superficial, because any central wave function (such as some Gaussians) would have been just as reasonable for the exploration. We explored the central wave function because suppressing the end-point singularities allows the regions of smaller  $b$  to contribute more effectively in the integrations. The results of the calculation with the central model are shown in Fig. 7. One sees a rapid rise of the transparency ratio with increasing  $Q^2$  with this model. This vindicates the correlation of a rising transparency ratio with short distance dominance.

These results support the following comment on the theoretical consistency of the perturbative treatment. Suppose a rapid rise of the transparency ratio with  $Q^2$  were observed: then a central model,  $A \gg 1$ , and the short-distance assumptions of the calculation, would all be internally consistent. This is in contrast to the free-space case, where unfortunately  $Q^2$  is not quite large enough to draw a similar conclusion, and nuclear filtering is absent. A naive interpretation that central models have been ruled out by free-space data also must be set aside as of questionable consistency. Suppose a flat dependence of the transparency ratio with  $Q^2$  were observed: then one can interpret it as evidence favoring the endpoint models, but with the same questionable consistency as in free space. If one is optimistic the nuclear case is slightly better in consistency, and then the flat  $Q^2$  dependence becomes a prediction of the end-point philosophy.

On the last optimistic basis, our calculations indicate that one might be able to learn more than previously thought possible about the internal structure of protons from the nuclear target data. There is a simple rule: If the transparency ratio rises quickly with  $Q^2$ , then the distribution amplitudes must be centrally peaked. If the transparency ratio rises slowly with  $Q^2$ , then it is consistent with strong end-point contributions.

## V. CONCLUSION

A primary uncertainty of color transparency calculations in the models used by other groups is the reliability of short-distance assertions of the hard scattering. Without that assertion, models of hadronic propagation cannot “divide out” the hard scattering. We do not grant the assertion of idealized short-distance, and (with all other calculations) find that contamination from long distance contributions in free-space is

“of order unity.” However we find that the long distance components of the amplitudes are considerably suppressed in the nuclear medium, compared to the same calculation in free space. This implies that perturbative QCD is better applied in the nuclear medium.

Using the end point dominated model of the distribution amplitude, for the case of the proton we find a slow rise in the transparency ratio for energies that can be probed in the future at CEBAF and ELFE. The pion, on the other hand, shows a very rapid increase. It has been known for some years that the rise with  $Q^2$  is not particularly definitive scientific standard [13]. Taking into account nuclear filtering, the slope measures compensation between two processes: One process tends to decrease the scattering rate: the purification of wave functions to short distance. The other feature of selecting increased short-distance increases survival of the struck hadron in propagation. We see this process of compensation quite clearly in our calculations, and find that it is a very general feature of PQCD. We therefore conclude that whether or not a rapid rise with  $Q^2$  is observed, the dependence on nuclear number  $A$  yields a characteristic curvature from which effective attenuation cross sections can be extracted.

Furthermore we find that models of distribution amplitudes that have wave functions more central in  $x$  automatically tend to have a greater short-distance component, generating a faster rise of the transparency ratio with  $Q^2$ . The slope of  $T(Q^2)$  may serve as a way to probe the fundamental quark wave functions. The distinction between distribution amplitudes which are end point dominated and more centrally dominated is very significant for the case of the proton. The end-point-dominated distribution amplitudes give very slow increase in transparency ratio as a function of  $Q^2$  and can be clearly confirmed or ruled out in upcoming experiments at CEBAF and ELFE.

## ACKNOWLEDGMENTS

We thank Bernard Pire, Stan Brodsky, Al Mueller and the organizers of the ELFE Workshop, St. Malo, for many insights and discussions in the early stages of this work. We also thank Hsiang-nan Li for many useful discussions. Financial support for this work was provided by the Board of Research in Nuclear Sciences (BRNS), the Crafoord Foundation and the DOE grant 85ER401214.

- 
- [1] S.J. Brodsky and G.R. Farrar, Phys. Rev. D **11**, 1309 (1975).
  - [2] S.J. Brodsky and G.P. Lepage, Phys. Rev. D **24**, 2848 (1981).
  - [3] V.L. Chernyak and A.R. Zhitnitsky, Phys. Rep. **112**, 173 (1984); Nucl. Phys. **B246**, 52 (1984).
  - [4] N. Isgur and C. Llewellyn-Smith, Phys. Rev. Lett. **52**, 1080 (1984).
  - [5] A.V. Radyushkin, Acta Phys. Pol. B **15**, 403 (1984); A.P. Bakulev and A.V. Radyushkin, Phys. Lett. B **271**, 223 (1991).
  - [6] J.P. Ralston and B. Pire, Phys. Rev. Lett. **61**, 1823 (1988).

- [7] J.P. Ralston and B. Pire, Phys. Rev. Lett. **65**, 2343 (1990).
- [8] P. Jain, B. Pire, and J.P. Ralston, Phys. Rep. **271**, 67 (1996).
- [9] S.J. Brodsky and A.H. Mueller, Phys. Lett. B **206**, 685 (1988).
- [10] S.J. Brodsky, in *Proceedings of the 13th International Symposium on Multiparticle Dynamics*, Vollandam, 1982, edited by W. Kittel *et al.* (World Scientific, Singapore, 1982); A.H. Mueller, in *Proceedings of the Rencontres de Moriond Les Arcs*, France, 1982, edited by J. Tran Thanh Van (Editions Frontiers, Gif-sur-Yvette, 1982).
- [11] A.S. Carroll *et al.*, Phys. Rev. Lett. **61**, 1698 (1988).

- [12] S.J. Brodsky and G.F. de Teramond, Phys. Rev. Lett. **60**, 1924 (1988).
- [13] P. Jain and J.P. Ralston, Phys. Rev. D **48**, 1104 (1993).
- [14] P. Jain, B. Kundu, and J.P. Ralston, hep-ph/0005126.
- [15] H. Gao and R.J. Holt, spokespersons, Jefferson Lab experiment E94-104.
- [16] H.-N. Li and G. Sterman, Nucl. Phys. **B381**, 129 (1992).
- [17] H.-N. Li, Phys. Rev. D **48**, 4243 (1993).
- [18] J. Bolz, R. Jakob, P. Kroll, M. Bergmann, and N.G. Stefanis, Z. Phys. C **66**, 267 (1995).
- [19] B. Kundu, H.-N. Li, J. Samuelsson, and P. Jain, Eur. Phys. J. C **8**, 637 (1999).
- [20] G.R. Farrar, H. Liu, L.L. Frankfurt, and M.I. Strikman, Phys. Rev. Lett. **61**, 686 (1988).
- [21] J.P. Blaizot, R. Venugopalan, and M. Prakash, Phys. Rev. D **45**, 814 (1992).
- [22] B.Z. Kopeliovich and B.G. Zakharov, Phys. Rev. D **44**, 3466 (1991).
- [23] B.K. Jennings and G.A. Miller, Phys. Lett. B **274**, 442 (1992); **318**, 7 (1993); Phys. Rev. C **49**, 2637 (1994).
- [24] P. Jain and J.P. Ralston, Phys. Rev. D **46**, 3807 (1992).
- [25] J.P. Ralston and B. Pire, in Proceedings of Second Workshop on Hadronic Physics with Electrons Beyond 10 GeV, Dourdan, France, 1990 [Nucl. Phys. **A532**, 155c (1991)].
- [26] J.P. Ralston and P. Jain, Nucl. Phys. **A622**, 166c (1997).
- [27] R.J. Glauber, in *Lectures in Theoretical Physics*, edited by W.E. Brittin and L.G. Dunham (Interscience, New York, 1959).
- [28] L. Durand and H. Pi, Phys. Rev. D **40**, 1436 (1989).
- [29] F.E. Low, Phys. Rev. D **12**, 163 (1975); S. Nussinov, Phys. Rev. Lett. **34**, 1286 (1975).
- [30] J.F. Gunion and D.E. Soper, Phys. Rev. D **15**, 2617 (1977).
- [31] H. De Vries, C.W. De Jager, and C. De Vries, At. Data Nucl. Data Tables **36**, 495 (1987).
- [32] G. Sterman and P. Stoler, Annu. Rev. Nucl. Part. Sci. **47**, 193 (1997).
- [33] C.E. Carlson and J. Milana, Phys. Rev. Lett. **65**, 1717 (1990).
- [34] E.D. Bloom and F.J. Gilman, Phys. Rev. Lett. **25**, 1140 (1970).
- [35] I.D. King and C.T. Sachrajda, Nucl. Phys. **B279**, 785 (1987).
- [36] A. Duncan and A.H. Mueller, Phys. Lett. **90B**, 159 (1980); Phys. Rev. D **21**, 1636 (1980).
- [37] T.-S.H. Lee and G.A. Miller, Phys. Rev. C **45**, 1863 (1992).
- [38] G.A. Miller and J.E. Spencer, Ann. Phys. (N.Y.) **100**, 562 (1976).
- [39] N. Makins *et al.*, Phys. Rev. Lett. **72**, 1986 (1994).
- [40] T.G. O'Neill *et al.*, Phys. Lett. B **351**, 87 (1995).
- [41] D. Abbott *et al.*, Phys. Rev. Lett. **80**, 5072 (1998).